International Journal of
Radiation Oncology
biology • physics

www.redjournal.org

Clinical Investigation: Thoracic Cancer

A Phase I Study of Chemoradiotherapy With Use of Involved-Field Conformal Radiotherapy and Accelerated Hyperfractionation for Stage III Non-Small Cell Lung Cancer: WJTOG 3305

Takuhito Tada, M.D.,[*,†] Yasutaka Chiba, M.D.,[‡] Kayoko Tsujino, M.D.,[§] Haruyuki Fukuda, M.D.,[‖] Yasumasa Nishimura, M.D.,[¶] Masaki Kokubo, M.D., Ph.D.,[**] Shunichi Negoro, M.D.,[††] Shinzoh Kudoh, M.D.,[‡‡] Masahiro Fukuoka, M.D.,[§§] Kazuhiko Nakagawa, M.D., Ph.D.,[‖‖] and Yoichi Nakanishi, M.D.[¶¶]

Departments of *Radiology and [‡‡]Respiratory Medicine, Osaka City University Graduate School of Medicine, Osaka; Departments of [†]Radiology and [§§]Medical Oncology, Izumi Municipal Hospital, Izumi; Departments of [‡]Environmental Medicine and Behavioural Science, [¶]Radiation Oncology, and [‖‖]Medical Oncology, Kinki University Faculty of Medicine, Osaka-sayama; Departments of [§]Radiation Oncology and [††]Medical Oncology, Hyogo Cancer Center, Akashi; [‖]Department of Radiology, Osaka Prefectural Medical Center for Respiratory and Allergic Diseases, Habikino; **Division of Radiation Oncology, Institute of Biomedical Research and Innovation, Kobe; and [¶¶]Research Institute for Disease of the Chest, Graduate School of Medical Science, Kyusyu University, Fukuoka, Japan

Received Jan 21, 2011, and in revised form May 19, 2011. Accepted for publication Jun 12, 2011

Summary

This phase I study of chemo-radiotherapy used involved-field conformal radiotherapy with accelerated Twice-daily hyperfractionation in patients with stage III non-small cell lung cancer. Although the dose of radiation was escalated to 72 Gy in 48 fractions, the maximum tolerated dose was not reached.

Purpose: A Phase I study to determine a recommended dose of thoracic radiotherapy using accelerated hyperfractionation for unresectable non–small-cell lung cancer was conducted.

Methods and Materials: Patients with unresectable Stage III non–small-cell lung cancer were treated intravenously with carboplatin (area under the concentration curve 2) and paclitaxel (40 mg/m^2) on Days 1, 8, 15, and 22 with concurrent twice-daily thoracic radiotherapy (1.5 Gy per fraction) beginning on Day 1 followed by two cycles of consolidation chemotherapy using carboplatin (area under the concentration curve 5) and paclitaxel (200 mg/m^2). Total doses were 54 Gy in 36 fractions, 60 Gy in 40 fractions, 66 Gy in 44 fractions, and 72 Gy in 48 fractions at Levels 1 to 4. The dose-limiting toxicity, defined as Grade $\geq$4 esophagitis and neutropenic fever and Grade $\geq$3 other nonhematologic toxicities, was monitored for 90 days.

Results: Of 26 patients enrolled, 22 patients were assessable for response and toxicity. When 4 patients entered Level 4, enrollment was closed to avoid severe late toxicities. Dose-limiting toxicities occurred in 3 patients. They were Grade 3 neuropathy at Level 1 and Level 3 and Grade 3 infection at Level 1. However, the maximum tolerated dose was not reached. The median survival time was 28.6 months for all patients.

Reprint requests to: Takuhito Tada, M.D., Department of Radiology, Izumi Municipal Hospital, 4-10-10 Fuchucho, Izumi City, 594-0071, Japan. Tel: (+81) 725411331; Fax: (+81) 725433350; E-mail: tada@msic.med.osaka-cu.ac.jp

Presented in part at the 52nd Annual Meeting of the American Society of Radiation Oncology, Oct 31 to Nov 4, 2010, San Diego, CA.

Conflict of interest: M. Kokubo is an advisor to Mitsubishi Heavy Industries Ltd. M. Fukuoka receives honoraria from Astrozeneca, Chugai Pharmaceutical Co., Boehringer Ingelheim, and Daiichisankyo. Y. Nakanishi receives research funding from Bristol-Myers. The authors declare no other conflict of interest.

Int J Radiation Oncol Biol Phys, Vol. 83, No. 1, pp. 327–331, 2012
0360-3016/$ - see front matter
doi:10.1016/j.ijrobp.2011.06.1991

Conclusions: The maximum tolerated dose was not reached, although the dose of radiation was escalated to 72 Gy in 48 fractions. However, a dose of 66 Gy in 44 fractions was adopted for this study because late toxicity data were insufficient.

Keywords: Non–small-cell lung cancer, Chemoradiation, Three-dimensional conformal radiotherapy, Accelerated hyperfractionation, Dose escalation

Introduction

For the treatment of locally advanced inoperable non–small-cell lung cancer (NSCLC), concurrent chemoradiotherapy has shown significantly better survival than sequential therapy (1–4). Even in concurrent chemoradiotherapy, however, locoregional control is unsatisfactory at a standard dose of 56 to 60 Gy (3, 5–7). To improve locoregional control, several dose escalation trials have been performed using three-dimensional (3D) planning techniques, and it has been suggested that 74 Gy is tolerable with concurrent or sequential chemotherapy (8–11).

In conventional fractionation, the benefits of dose escalation are considered limited. Irradiation at a dose of 74 Gy in conventional fractionation requires more than 7 weeks. Even at standard doses, accelerated repopulation is induced during the later part of radiation therapy and is a cause of radiation failure (12). When the treatment time is prolonged, the influence of accelerated repopulation becomes more evident.

Therefore, dose escalation without prolonged treatment time is supposed to bring better outcome, and accelerated hyperfractionation seems to be an effective strategy for shortening treatment time. As the first step to verify the hypothesis, the West Japan Thoracic Oncology Group designed a Phase I trial to define the maximum tolerated dose (MTD) of 3D conformal radiotherapy (CRT) using accelerated hyperfractionation in NSCLC patients.

Methods and Materials

Eligibility

The patient eligibility was as follows: histologic or cytologic diagnosis of NSCLC, unresectable Stage IIIA or IIIB disease, age less than 75 years, Eastern Cooperative Oncology Group performance score of 0 to 1, and function as shown by laboratory determinations including leukocyte count of at least 4,000/mm^3, hemoglobin concentration of at least 9.5 g/dL, platelet count of at least 100,000/mm^3, aspartate aminotransferase and alanine aminotransferase of 2.0 times the upper limit of normal range or less, serum total bilirubin of 1.5 mg/dL or less, serum creatinine of 1.5 mg/dL or less, and PaO_2 at rest of at least 70 mm Hg.

The patients were ineligible if they met any of the following criteria: supraclavicular nodal metastases, interstitial pneumonitis or pulmonary fibrosis, prior thoracic radiation therapy, malignant pleural effusion or malignant pericardial effusion, active concomitant malignancy or recent (<3 years) history of any malignancy, or other serious concomitant medical conditions. The study protocol was approved by each institutional review board for clinical use. All patients gave written informed consent before enrollment.

Patient assessment

All patients underwent a complete medical history and physical examination. Imaging studies, including chest X-ray, computed tomography of the chest and upper abdomen, computed tomography or magnetic resonance imaging of the brain, and positron emission tomography, were required.

Treatment schedule

The patients received concurrent chemoradiotherapy using accelerated hyperfractionation. On Days 1, 8, 15, and 22, carboplatin (area under the concentration curve 2 using the Calvert equation) and paclitaxel (40 mg/m^2) were administered intravenously.

After the concurrent chemoradiotherapy, the patients received two cycles of consolidation chemotherapy consisting of carboplatin (area under the concentration curve 5) and paclitaxel (200 mg/m^2) with an interval of 3 weeks. The first cycle of consolidation chemotherapy was begun 4 weeks after the concurrent chemoradiotherapy, if leukocyte count was at least 4,000/mm^3, platelet count at least 100,000/mm^3, aspartate aminotransferase and alanine aminotransferase 2.0 times the upper limit of normal range or less, serum total bilirubin 1.5 mg/dL or less, serum creatinine 1.5 mg/dL or less, and Eastern Cooperative Oncology Group performance score of 0 to 2. The subsequent cycle of consolidation chemotherapy was repeated if leukocyte count was at least 3,000/mm^3, neutrophil count at least 1,500/mm^3, platelet count at least 100,000/mm^3, serum creatinine 1.5 mg/dL or less, and body temperature not exceeding 38°C.

The 3D CRT began on Day 1. Irradiation was performed with 4-MV or higher photons from a linear accelerator. Patients received 1.5 Gy per fraction twice daily with at least a 6-hour interval between each fraction.

Target volume definitions

Elective nodal irradiation was not performed. The gross tumor volume (GTV) was defined as the volume occupied by visible disease. The GTV included the primary tumor and involved lymph nodes measuring larger than 1.0 cm (short axis measurement) or lymph nodes with a diameter of 5 mm or more as shown by positron emission tomography. The clinical target volume (CTV) was defined as the GTV of the primary tumor plus a margin of 5 mm for all borders and GTV of the lymph nodes without a margin. The planning target volume (PTV) was the CTV plus an adequate margin added to compensate for variability in treatment setup, breathing, or motion during treatment. In

general, the PTV included the CTV plus 1.0 cm of expansion at all borders.

Tissue inhomogeneity corrections were used. The volume of both lungs that received more than 20 Gy should not exceed 35% of the total lung, and the maximum dose to the spinal cord could not exceed 45 Gy. It was desirable but not required that the PTV receive more than 93% but less than 107% of its prescribed dose. After the dose of 36 Gy was reached, the PTV could be reduced after shrinkage of the GTV.

Dose escalation

The MTD was defined as the dose at which 3 or more of 6 patients experienced a dose-limiting toxicity (DLT). The DLT was defined as Grade 4 or more esophagitis, neutropenic fever, dermatitis, or nausea/vomiting and other Grade 3 or more nonhematologic toxicity. Furthermore, interruption of irradiation for more than 2 weeks was also defined as a DLT. The DLT was monitored for 90 days.

Irradiation was performed for 5 days per week. The prescribed doses were 54 Gy in 36 fractions over 3.6 weeks, 60 Gy in 40 fractions over 4.0 weeks, 66 Gy in 44 fractions over 4.4 weeks, and 72 Gy in 48 fractions over 4.8 weeks (Levels 1–4). When the DLT was observed in 0 of 4 patients, in $\leq$1 of 5 patients, or in $\leq$2 of 6 patients at each level, the radiation dose was to be escalated.

Evaluation

The Response Evaluation Criteria in Solid Tumors were used for response assessment (13). Toxicity was evaluated according to the National Cancer Institute Common Toxicity Criteria (version 3.0). An extramural review was conducted to validate the eligibility of the patients and staging.

The duration of survival was counted from the day of entry to the study, and the overall survival was calculated according to the Kaplan-Meier method (14).

Results

Patients' characteristics

Between April 2006 and April 2008, 26 patients were enrolled in this study. Four patients were excluded because of allergic reactions to paclitaxel on Day 1 (n = 1), cerebral infarction on Day 2 (n = 1), and supraclavicular nodal metastases (n = 2). The remaining 22 patients were included in the analysis. They were 6, 7, 5, and 4 patients at Levels 1 through 4, respectively. Although, as a rule, 4 to 6 patients were enrolled in each level, 1 patient was increased at Level 2 because the sixth and seventh patients enrolled at the same time. The baseline characteristics of the 22 patients are summarized in Table 1.

When 4 patients entered Level 4, enrollment was closed to avoid severe late toxicities in the esophagus and the bronchia.

Treatment administration

All patients received full doses of radiation therapy, and interruption of radiation therapy was required in only 4 patients.

Table 1 Patient characteristics (n = 22)

Characteristics	n	%
Age (y)		
Median		63
Range		45–70
Sex		
M	19	86
F	3	14
ECOG performance status		
0	7	32
1	15	68
Histology		
Squamous cell carcinoma	10	45
Adeno carcinoma	10	45
Large cell carcinoma	0	0
Others	2	10
Stage		
IIIA	11	50
IIIB	11	50

Abbreviation: ECOG = Eastern Cooperative Oncology Group.

Interruptions ranged from 1 day to 7 days. All patients received four cycles of concurrent chemotherapy, and 19 patients (86%) received two cycles of consolidation chemotherapy.

Toxicity

The major toxicities are summarized in Table 2.

The DLTs occurred in 3 patients. Two cases of Grade 3 neuropathy were observed, one at Level 1 and the other at Level 3, and one case of Grade 3 infection occurred at Level 1. Furthermore, Grade 5 radiation pneumonitis was observed at Level 1; however, it was not treated as a DLT because the event occurred after the observation period of 90 days. Grade 3 esophagitis was observed in 3 patients, 1 at Level 3 and the others at Level 4. Grade 3 esophagitis and nausea were not defined as DLTs.

At Level 4, no DLT occurred in the 4 patients. Therefore, the MTD was not reached in the present study.

Response and survival

The figure shows the overall survival. The median survival time was 28.6 months for all patients and 30.2 months for patients who received more than 60 Gy. The response rate was 77% for all patients.

Patterns of relapse

Table 3 shows the first sites of relapse. Of 11 patients with locoregional relapse, 1 had upper mediastinal lymph node metastasis, which was located out of the radiation portal. Of 5 patients with distant metastasis, 3 had lung metastasis.

Discussion

With the use of 3D planning techniques, several dose escalation trials have been performed. Kong *et al.* reported that doses of CRT

Table 2 Major toxicities (n = 22)

Toxicity	Grade 3		Grade 4		Grade 5	
	n	%	n	%	n	%
Hematologic						
Leukopenia	16	73	1	5		
Neutropenia	5	23	12	55		
Anemia	2	9	0	0		
Thrombocytopenia	0	0	0	0		
Nonhematologic						
Neuropathy	2	9	0	0	0	0
Infection	1	5	0	0	0	0
Pneumonitis	0	0	0	0	1	5
Esophagitis	3	14	0	0	0	0
Nausea	1	5	0	0	0	0

could be escalated up to 103 Gy for smaller tumors (15). However, the 5-year local control rates were only 49% even at 92 to 103 Gy and 35% at 74 to 84 Gy. The insufficient local control indicated limitation of dose escalation in conventional fractionation and warranted further exploration for different strategies.

A risk of severe late toxicities, such as esophageal stenosis and bronchial occlusion, was predicted from the beginning of the study. After that, experience with Levels 1 through 3 indicated that prescription of high doses in the esophagus or the main bronchi was inevitable in most patients. Therefore, enrollment was closed in the middle of Level 4 to avoid severe late toxicities. Emami *et al.* reported that in treatment of the esophagus, the tolerance dose that would result in a 50% probability of complications within 5 years of treatment was 72 Gy (16). However, data on tolerance doses by accelerated hyperfractionation are lacking. Therefore, careful long-term follow-up of the present study is required. Recently, Atsumi *et al.* reported that the severity and frequency of esophageal stenosis after radiation therapy were greater in patients with esophageal cancer with full circumference involvement and increased with esophageal wall thickness (17). The tolerance dose for the esophagus might be higher in patients without esophageal cancer than in those with esophageal cancer.

In radiation therapy using accelerated hyperfractionation, acute esophagitis is a toxicity of particular concern. In the present study, 3 patients experienced Grade 3 esophagitis: 2 of 4 patients at Level 4, but only 1 patient at Levels 1 through 3 (n = 18). The

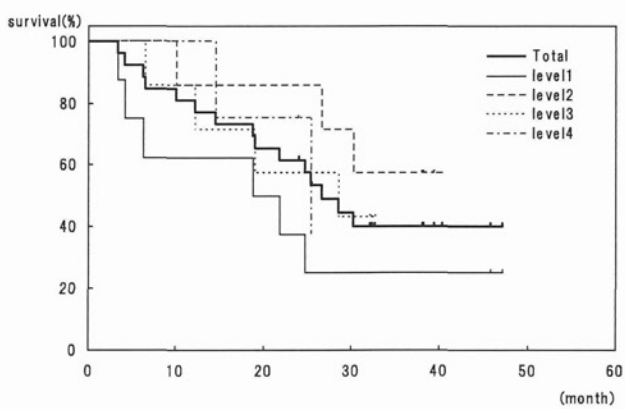

Fig. Kaplan-Meier survival curves for all patients and for patients in Levels 1–4. The median survival time was 28.6 months for all patients.

Table 3 Site of first failure (n = 22)

Site	n	%
Progression free	9	41
Locoregional alone	8	36
Locoregional and distant	3	14
Distant*	5	23
Lung	3	14
Brain	1	5
Small intestine	1	5

* Distant includes locoregional and distant, and distant alone.

low frequency of esophagitis has often been observed in other Japanese trials (18, 19). The causes of this phenomenon are not well known. One possible explanation is differences in ethnic background. Twice-daily CRT with a dose of 1.3 to 1.45 Gy per fraction could be recommended in patients with other ethnic backgrounds, if this regimen is shown to bring a better outcome.

Another toxicity of concern is radiation pneumonitis. In the present study, Grade 5 radiation pneumonitis was observed in 1 patient. In other patients, however, Grade 3 or more radiation pneumonitis was not observed. Some radiation pneumonitis is inevitable to some degree, and the frequency of Grade 3 or more pneumonitis was rather low in the present study. Tsujino *et al.* reported a decreased incidence of radiation pneumonitis by accelerated hyperfractionation in the treatment of limited-stage small-cell lung cancer, although initially they expected that accelerated hyperfractionation would increase the incidence and severity of radiation pneumonitis (20). The results in the present study are consistent with those reported by Tsujino *et al.*

The DLTs observed in the current study were Grade 3 neuropathy and Grade 3 infection. They were mainly caused by chemotherapy. By contrast, Grade 5 radiation pneumonitis was not treated as a DLT because it occurred after the observation period of 90 days. The definition of DLT used in this study was probably inadequate for a radiation dose escalation study. Chemotherapy-induced toxicities should be given less consideration, and those caused by radiation therapy should be more strictly weighed.

The cutoff of 90 days for the observation period of DLTs was considered not sufficient. However, the observation period could not be more prolonged because the Phase I study had to be completed within a suitable time. Toxicities were evaluated after the observation period. In recent Phase I studies, the observation period was defined similarly (21–23).

Although the number of patients was relatively small in the present study, the method of assigning 6 patients to each dose bin is an option in a Phase I study (21). However, the data about survival were not reliable because of the small sample size. The data are to be verified in the following Phase II study.

In the present study, the dose of CRT was escalated to 72 Gy in 48 fractions, and MTD was not reached. In principle, 72 Gy should be the recommended dose. However, late toxicity data are insufficient, and enrollment was closed in the middle of Level 4. Furthermore, on the basis of our experience with the treatment of small-cell lung cancer, CRT with a dose of 66 Gy in accelerated hyperfractionation brings better local control than 74 Gy in conventional fractionation, which was defined as a recommended dose in several trials. The favorable median survival time of 30.2 months for patients who received 60 to 72 Gy in the present study is consistent with our experience. Therefore, a dose of 66 Gy in 44 fractions was adopted in the present study. On the basis

of the results presented here, we are currently preparing a Phase II study.

In conclusion, the MTD was not reached in the present study, although the dose of radiation was escalated to 72 Gy in 48 fractions. Acute toxicities were relatively mild. However, a dose of 66 Gy in 44 fractions was adopted for the present study because late toxicity data were insufficient.

References

1. Furuse K, Fukuoka M, Kawahara M, *et al.* Phase III study of concurrent versus sequential thoracic radiotherapy in combination with mitomycin, vindesine, and cisplatin in unresectable stage III non-small cell lung cancer. *J Clin Oncol* 1996;17:2692–2699.
2. Fournel P, Robinet G, Thomas P, *et al.* Randomized phase III trial of sequential chemoradiotherapy compared with concurrent chemo-radiotherapy in locally advanced non-small-cell lung cancer: Group Lyon-Saint-Etienne d'Oncologie Thoracique-Groupe Francais de Pneumo-Cancerogie NPC 95-01 Study. *J Clin Oncol* 2005;23: 5910–5917.
3. Zatloukal P, Petruzelka L, Zemanova M, *et al.* Concurrent versus sequential chemoradiotherapy with cisplatin and vinorelbine in locally advanced non-small cell lung cancer: A randomized study. *Lung Cancer* 2004;46:87–98.
4. Curran W, Scott C, Langer C, *et al.* Long term benefit is observed in a phase III comparison of sequential vs concurrent chemo-radiation for patients with unresectable stage III NSCLC: RTOG 9410. *Proc Am Soc Clin Oncol* 2003;22:621 (abstr 2499).
5. Schaake-Koning C, Vand den Bogaert W, Dalesio O, *et al.* Effect of concomitant cisplatin and radiotherapy on inoperable non-small-cell lung cancer. *N Engl J Med* 1992;326:524–530.
6. Tada T, Minakuchi K, Matsui K, *et al.* A single institutional subset analysis of the WJLCG study comparing concurrent and sequential chemoradiotherapy for stage III non-small-cell lung cancer. *Radiat Med* 2004;22:163–167.
7. Le Chevalier T, Arriagada R, Tarayre M, *et al.* Significant effect of adjuvant chemotherapy on survival in locally advanced non-small-cell lung carcinoma [Letter]. *J Natl Cancer Inst* 1992;84:58.
8. Socinski MA, Rosenmann JG, Halle JS, *et al.* Induction carboplatin/paclitaxel followed by concurrent carboplatin/paclitaxel and dose-escalating conformal thoracic radiation therapy in unresectable stage IIIA/B non-small cell lung cancer: A modified phase I trial. *Cancer* 2000;89:534–542.
9. Rosenmann JG, Halle JS, Socinski MA, *et al.* High dose conformal radiotherapy for treatment of stage IIIA/IIIB non-small-cell lung cancer: Technical issues and results of a phase I/II trial. *Int J Radiat Oncol Biol Phys* 2002;54:348–356.
10. Blackstock AW, Lesser GJ, Fletcher-Steede J, *et al.* Phase I study of twice-weekly gemcitabin and concurrent thoracic radiation for patients with locally advanced non-small-cell lung cancer. *Int J Radiat Oncol Biol Phys* 2001;51:1281–1289.
11. Blackstock AW, Ho C, Butler J, *et al.* Phase Ia/Ib chemo-radiation trial of gemcitabin and dose-escalated thoracic radiation in patients with stage III A/B non-small cell lung cancer. *J Thorac Oncol* 2006; 1:434–440.
12. Withers HR, Taylor JMG, Maciewjewski B, *et al.* The hazard of accelerated tumor clonogen repopulation during radiotherapy. *Acta Oncol* 1988;27:131–146.
13. Therasse P, Arbuck SG, Eisenhauer EA, *et al.* New guidelines to evaluate the response to treatment in solid tumors. *J Natl Cancer Inst* 2000;92:205–216.
14. Kaplan EL, Meier P. Nonparametric estimation from incomplete evaluations. *J Am Stat Assoc* 1958;53:457–481.
15. Kong FM, Haken RKT, Schipper MJ, *et al.* High dose radiation improved local tumor control and overall survival in patients with inoperable/unresectable non-small-cell lung cancer: Long-term results of a radiation dose escalation study. *Int J Radiat Oncol Biol Phys* 2005;63:324–333.
16. Emami B, Lyman J, Brown A, *et al.* Tolerance of normal tissue to therapeutic irradiation. *Int J Radiat Oncol Biol Phys* 1991;21: 109–122.
17. Atsumi K, Shioyama Y, Nakamura K, *et al.* Predictive factors of esophageal stenosis associated with tumor regression in radiation therapy for locally advanced esophageal cancer. *J Radiat Res* 2010;51: 9–14.
18. Saito H, Takada Y, Ichinose Y, *et al.* Phase II study of etoposide and cisplatin with concurrent twice-daily thoracic radiotherapy followed by irinotecan and cisplatin in patients with limited-disease small-cell lung cancer: West Japan Thoracic Oncology Group 9902. *J Clin Oncol* 2006;24:5247–5252.
19. Takada M, Fukuoka M, Kawahara M, *et al.* Phase III study of concurrent versus sequential thoracic radiotherapy in combination with cisplatin and etoposide for limited-stage small-cell lung cancer: Results of the Japan Clinical Oncology Group Study 9104. *J Clin Oncol* 2002;20:3054–3060.
20. Tsujino K, Hirota S, Kotani Y, *et al.* Radiation pneumonitis following concurrent accelerated hyperfractionated radiotherapy and chemotherapy for limited-stage small-cell lung cancer: Dose-volume histogram analysis and comparing with conventional chemoradiation. *Int J Radiat Oncol Biol Phys* 2006;64:1100–1105.
21. Schild SE, McGinnis WL, Graham D, *et al.* Results of a phase I trial of concurrent chemotherapy and escalating doses of radiation for unresectable non-small-cell lung cancer. *Int J Radiat Oncol Biol Phys* 2006;65:1106–1111.
22. Nishimura Y, Nakagawa K, Takeda K, *et al.* Phase I/II trial of sequential chemoradiotherapy using novel hypoxic cell radiosensitizer, doranidazole (PR-350), in patients with locally advanced non-small-cell lung cancer (WJTOG-0002). *Int J Radiat Oncol Biol Phys* 2007;69: 786–792.
23. Marks LB, Garst J, Socinsky MA, *et al.* Carboplatin/paclitaxel or carboplatin/vinorelbine followed by accelerated hyperfractionated conformal radiation therapy: Report of a prospective phase I dose escalation trial from the Carolina conformal therapy consortium. *Clin Oncol* 2004;22:4329–4340.

A Novel Mass Spectrometry–Based Assay for Diagnosis of *EML4-ALK*–Positive Non–Small Cell Lung Cancer

Kazuko Sakai, PhD, Isamu Okamoto, MD, PhD,† Ken Takezawa, MD, PhD,† Tomonori Hirashima, MD,‡ Hiroyasu Kaneda, MD, PhD,† Masayuki Takeda, MD, PhD,† Kazuko Matsumoto, MD, PhD,* Hideharu Kimura, MD, PhD,* Yoshihiko Fujita, PhD,* Kazuhiko Nakagawa, MD, PhD,† Tokuzo Arao, MD, PhD,* and Kazuto Nishio, MD, PhD**

Introduction: The presence of the transforming fusion gene echinoderm microtubule-associated protein–like 4 (*EML4*)–anaplastic lymphoma kinase (*ALK*) in non–small-cell lung cancer (NSCLC) is a predictive marker for the efficacy of anaplastic lymphoma kinase inhibitors. However, the currently available assays for the detection of the different variants of *EML4-ALK* have limitations.

Methods: We developed an assay system for the detection of *EML4-ALK* variants 1, 2, 3a, 3b, 4, 5a, 5b, 6, or 7 transcripts in total RNA obtained from formalin-fixed, paraffin-embedded (FFPE) specimens of NSCLC tissue. The assay is based on region-specific polymerase chain reaction amplification of *EML4-ALK* complementary DNA followed by specific single-base primer extension and analysis of the extension products by matrix-assisted laser desorption/ionization–time of flight mass spectrometry. The assay was validated by fluorescence in situ hybridization and the results confirmed by subcloning and sequencing of polymerase chain reaction products.

Results: Evaluation of the analytic sensitivity of the assay with serial dilutions of plasmids containing *EML4-ALK* complementary DNA sequences revealed it to be capable of the reliable detection of one copy of each plasmid per reaction. The assay also detected *EML4-ALK* variants 1 or 3 in three FFPE samples of surgically resected NSCLC shown to be positive for anaplastic lymphoma kinase rearrangement by fluorescence in situ hybridization. Furthermore, the assay identified variant 1 of *EML4-ALK* in 3 of 20 FFPE biopsy samples from patients with advanced NSCLC. All positive samples were confirmed by subcloning and sequencing.

Conclusions: Our novel assay is highly sensitive and effective for the detection of *EML4-ALK* in FFPE specimens.

Key Words: EML4-ALK, Non–small cell lung cancer, Paraffin-embedded tissue, Mass spectrometry, Diagnosis.

(*J Thorac Oncol.* 2012;7: 913–918)

*Department of Genome Biology and †Department of Medical Oncology, Kinki University, Faculty of Medicine, Osaka-Sayama, Osaka, Japan; and ‡Department of Thoracic Malignancy, Osaka Prefectural Medical Center for Respiratory and Allergic Diseases, Habikino-shi, Osaka, Japan.

Conflict of interest: The authors declare no conflict of interest.

Address for correspondence: Kazuto Nishio, MD, PhD, Kinki University Faculty of Medicine, Ohnohigashi 377-2, Osaka-sayama, Osaka, Japan. E-mail: knishio@med.kindai.ac.jp

ISSN: 1556-0864/12/913-918

Echinoderm microtubule-associated protein–like 4 (EML4)–anaplastic lymphoma kinase (ALK) was recently identified as a transforming fusion protein in lung cancer.[1] Both *EML4* and *ALK* genes are located on the short arm of chromosome 2. Multiple variants of *EML4-ALK* have been identified, with all variants including the same cytoplasmic portion of ALK but different portions of EML4 (with truncations at exons 2, 6, 13, 14, 15, 18, and 20).[2–4] The most common *EML4-ALK* variants are 1 and 3, which together account for ~60% of *EML4-ALK*–positive cases of non–small cell lung cancer (NSCLC).[5] Crizotinib, an inhibitor of the tyrosine kinase activity of ALK and MET (hepatocyte growth factor receptor), has been shown to be effective for the treatment of lung cancer patients harboring *EML4-ALK*.[6] Indeed, crizotinib was recently approved by the U.S. Food and Drug Administration for the treatment of advanced NSCLC in patients with an abnormal *ALK* gene.

The *EML4-ALK* translocation occurs in 5 to 10% of lung cancer patients.[1,2,7–10] Several assays have been developed for the detection of this translocation in clinical samples.[2,4,11] However, all of these assays have limitations with regard to sensitivity or the reliance on specialized techniques, with the development of higher-sensitivity assays based on simple methods being warranted.

MATERIALS AND METHODS

Plasmid Construction

Plasmids based on pCR2.1 or pcDNA3.1(+) and containing *EML4-ALK* or *ALK* complementary DNA (cDNA) were constructed as positive controls by TA cloning (Invitrogen, Madison, WI) or In-Fusion PCR cloning (Clontech, Palo Alto, CA).[12] Details of plasmid construction and corresponding primer sequences are provided in Supplemental Digital Content 1 (http://links.lww.com/JTO/A219) and 2 (http://links.lww.com/JTO/A220).

Clinical Samples

Formalin-fixed, paraffin-embedded (FFPE) samples were obtained from NSCLC patients who had undergone surgery or biopsy for the purpose of diagnosis at Kinki University Hospital. The study was approved by the Institutional Review Board with the conditions that samples

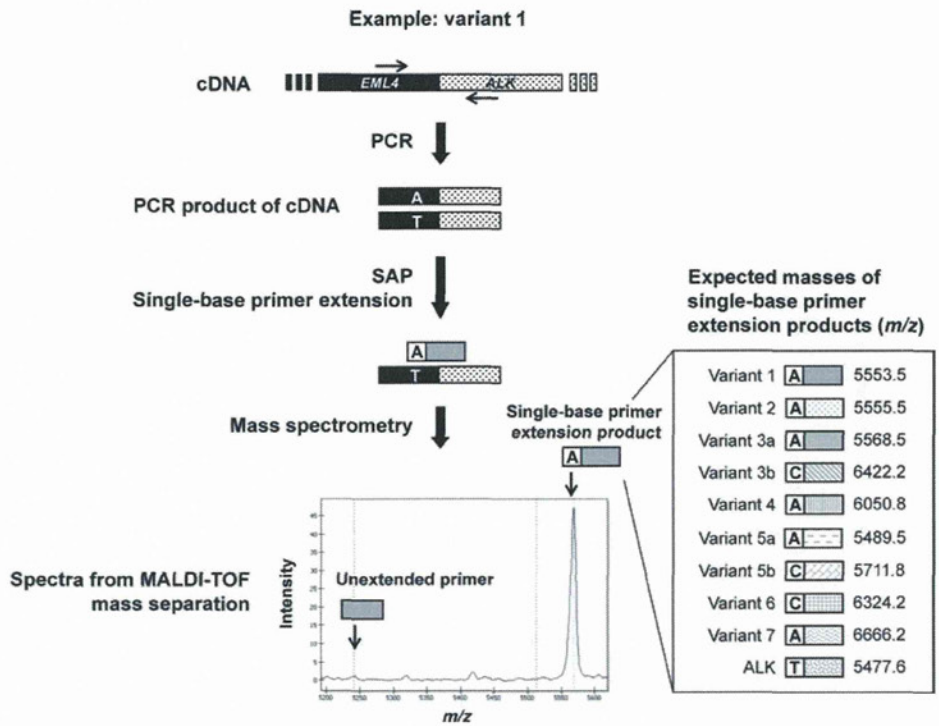

FIGURE 1. MassARRAY method for the detection of *EML4-ALK*. The region of *EML4-ALK* complementary DNA containing the fusion point is amplified by polymerase chain reaction (PCR), with the amplicons ranging in size from 70 to 130 bp. After dephosphorylation of the 5′ terminus of the PCR products with the use of shrimp alkaline phosphatase, a single-base primer extension reaction is performed. The primer extension products are then analyzed by matrix-assisted laser desorption ionization–time of flight mass spectrometry . The single-base extension reaction occurs only when an *EML4-ALK* fusion product is present in the sample.

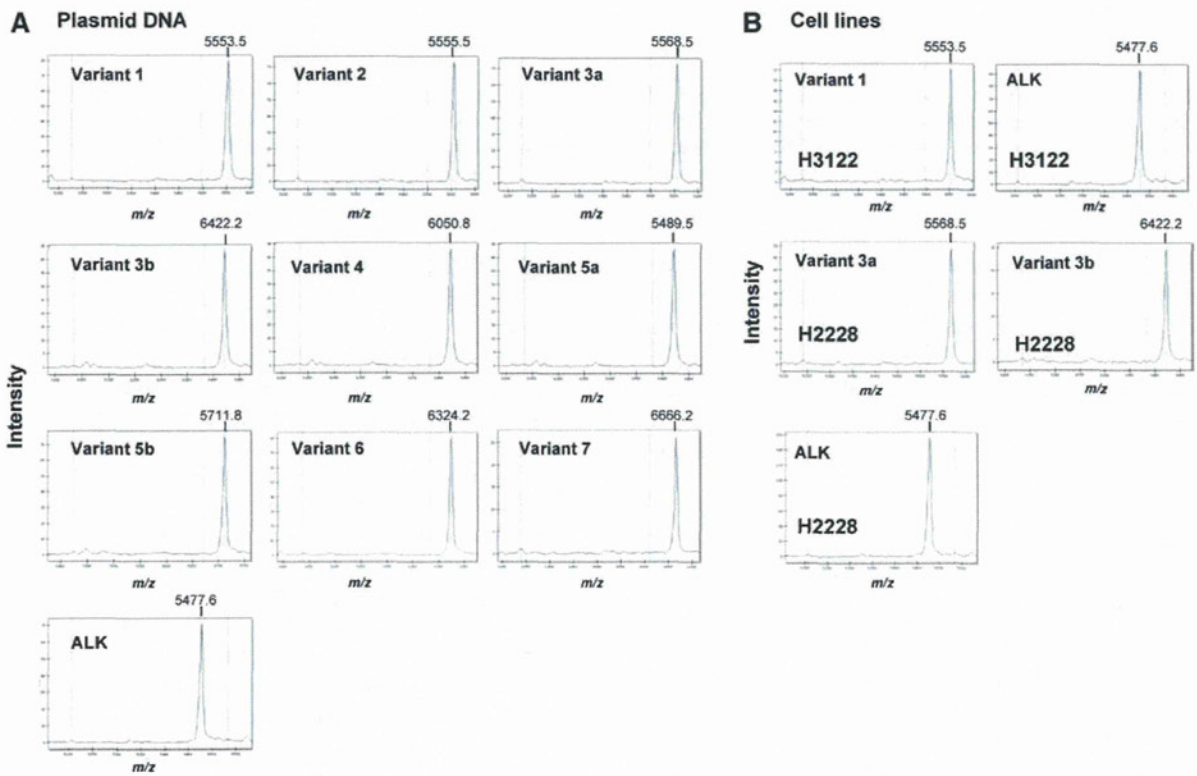

FIGURE 2. Representative spectra for *EML4-ALK* variants. Plasmid DNA (1 ng per reaction) containing the indicated variants of *EML4-ALK* (*A*) or total complementary DNA (5 ng per reaction) prepared from H3122 or H2228 cell lines (which harbor *EML4-ALK* variant 1 and variants 3a and 3b, respectively) (*B*) was subjected to the MassARRAY assay. Representative spectra for extension products between ~5100 and ~6800 Da are shown. The expected *m/z* values for each single-base extension product are as indicated in Figure 1. Three independent experiments were performed in triplicate with identical results.

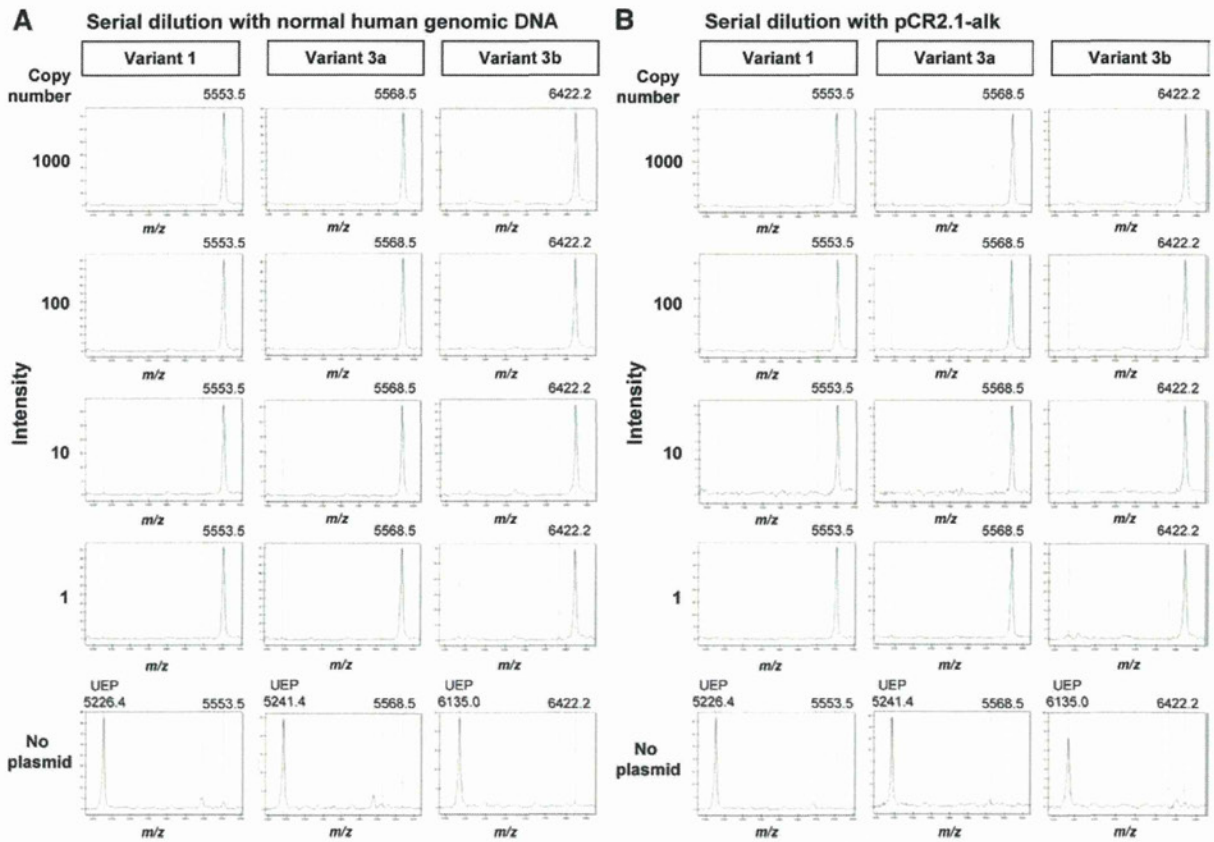

FIGURE 3. Sensitivity of *EML4-ALK* detection in plasmid DNA. The indicated copy numbers of pcDNA3.1(+) containing variants 1, 3a, or 3b of *EML4-ALK* were assayed in the presence of 1 ng of normal human genomic DNA (*A*) or 10 pg of pCR2.1-alk plasmid DNA (*B*). The copy number of plasmid DNA per reaction was calculated according to the formula: $6.022 \times 10^{23} \times$ [mass of DNA (g)]/[plasmid size (bp) $\times$ 660]. Three independent experiments were performed in triplicate with identical results. UEP, unextended primer.

be processed anonymously and analyzed for gene expression and that the study be disclosed publicly, according to the Ethical Guidelines for Human Genome Research published by the Ministry of Education, Culture, Sports, Science, and Technology, the Ministry of Health, Labor, and Welfare, and the Ministry of Economy, Trade, and Industry of Japan. The study also conforms to the provisions of the Declaration of Helsinki.

Cell Lines

The human NSCLC cell lines H2228 and H3122 were kindly provided by Dr. P. A. Jänne (Department of Medical Oncology, Dana-Farber Cancer Institute, Boston, MA). Short tandem repeat analysis was performed with genomic DNA isolated from H2228 and H3122 cells. The DNA profile of H2228 cells matched that in the American Type Culture Collection short tandem repeat database. The cells were maintained under a humidified atmosphere of 5% CO_2 at 37°C in RPMI 1640 medium (Sigma, St. Louis, MO) supplemented with 10% heat-inactivated fetal bovine serum (Equitech-Bio, Kerrville, TX).

Sample Processing

Total RNA was extracted from cell lines and FFPE samples with the use of an RNeasy Mini Kit (Qiagen, Valencia, CA) and an RNeasy FFPE Kit (Qiagen), respectively. The percentage of tumor cells in each FFPE specimen was evaluated by hematoxylin-eosin staining and found to be >10%. The isolated RNA was subjected to reverse transcription (RT) with the use of a High Capacity cDNA Reverse Transcription Kit (Applied Biosystems, Foster City, CA), and the resulting cDNA was stored at –80°C until analysis.

Detection of *EML4-ALK*

We used the MassARRAY iPLEX platform (Sequenom, San Diego, CA) for detection of *EML4-ALK*. The MassARRAY system involves a three-step process consisting of polymerase chain reaction (PCR), single-base primer extension, and separation of the products on a matrix-loaded silicon chip by matrix-assisted laser desorption ionization (MALDI)–time of flight (TOF) mass spectrometry (MS) (Fig. 1). PCR and the single-base primer extension reactions were performed in a thermal cycler (ABI-9700 instrument, Applied Biosystems), and the extension products were analyzed using the MALDI–TOF MS

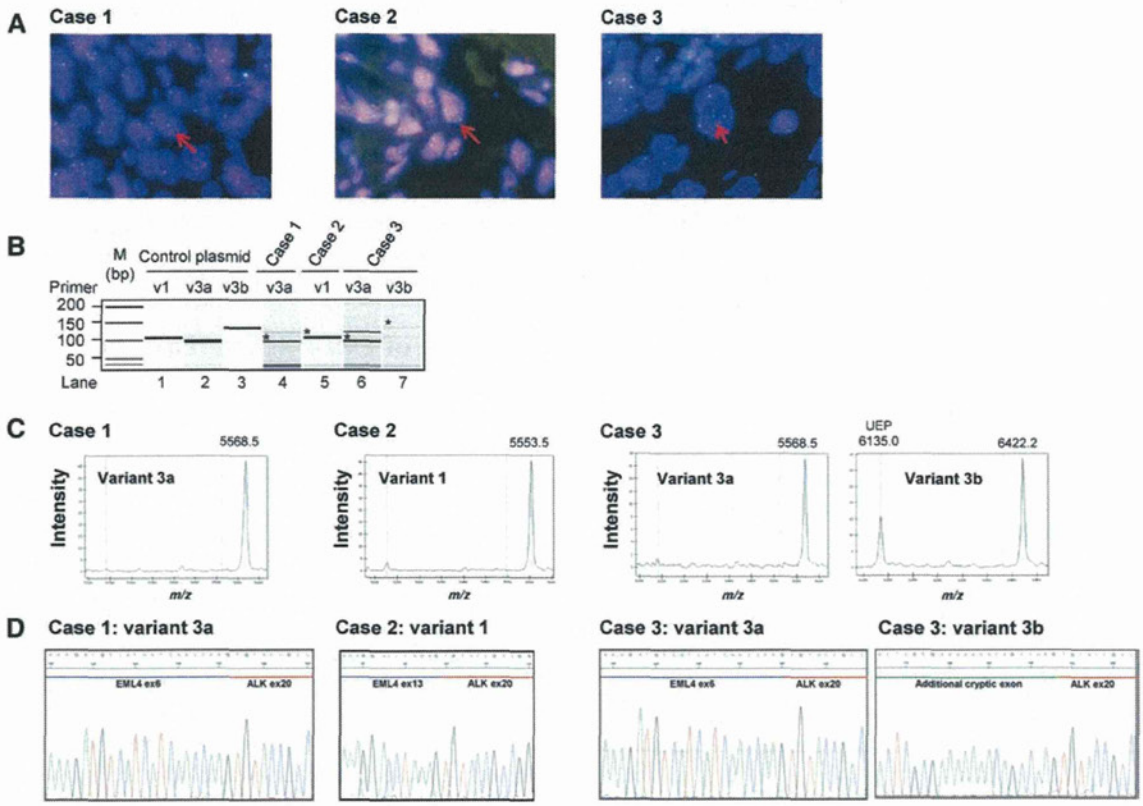

FIGURE 4. Detection of *EML4-ALK* in formalin-fixed, paraffin-embedded (FFPE) samples of surgically resected non–small cell lung cancer tissue. (*A*) Clinical specimens were subjected to fluorescence in situ hybridization analysis with differentially labeled probes for the 5′ (green) or 3′ (red) regions of the *ALK* locus. A pair of split signals (arrows) indicates the rearranged *ALK* locus. (*B*) polymerase chain reaction (PCR) products derived with PCR primer sets in the MassARRAY assay were separated with the use of an Agilent 2100 Bioanalyzer and a DNA 1000 LabChip Kit (Agilent Technologies, Inc., Palo Alto, CA). The PCR products are from pcDNA3.1(+)-v1 (lane 1), pcDNA3.1(+)-v3a (lane 2), pcDNA3.1(+)-v3b (lane 3), case 1 (lane 4), case 2 (lane 5), and case 3 (lanes 6 and 7). The asterisk indicates the corresponding band in each case. (*C*) Total RNA (10 ng) isolated from the FFPE samples in (*A*) was analyzed by the MassARRAY assay. Representative spectra are shown. The experiment was repeated twice with identical results. (*D*) The PCR products from (*C*) were also subcloned and sequenced. ex, exon.

(Sequenom). Detailed procedures and corresponding primer sequences are provided in Supplemental Digital Content 1 (http://links.lww.com/JTO/A219) and 3 (http://links.lww.com/JTO/A221), respectively.

Sequencing Analysis

PCR products were subcloned into the TOPO TA pCR2.1 vector (Invitrogen) and sequenced with an automated sequencer (ABI Prism 3100 Genetic Analyzer, Applied Biosystems) with the use of M13 universal primers.

Fluorescence In Situ Hybridization Analysis

FFPE tissue sectioned at a thickness of 4 μm and placed on glass slides was subjected to fluorescence in situ hybridization (FISH) with a break-apart probe for the *ALK* gene (Vysis LSI ALK Dual Color, Break Apart Rearrangement Probe; Abbott Molecular, Des Plaines, IL). FISH positivity was defined as the presence of >15% split signals in tumor cells.

RESULTS

Detection of *EML4-ALK* Variants

We developed an assay system based on the MassARRAY platform for the detection of *EML4-ALK* variants in NSCLC tissue (Fig. 1). The MassARRAY assay detected plasmid DNA corresponding to nine different *EML4-ALK* variants and wild-type *ALK* (Fig. 2*A*). Appropriate mass spectra for the single-base extension products were thus obtained (Figs. 1 and 2*A*). We next attempted to detect *EML4-ALK* in the human NSCLC cell lines H3122 and H2228, which harbor *EML4-ALK* variants 1 and 3, respectively.[7] The RT-PCR products of total RNA isolated from the cell lines were subjected to the MassARRAY assay. *EML4-ALK* variant 1 was detected in H3122 cells, whereas variants 3a and 3b were detected in H2228 cells (Fig. 2*B*). Wild-type *ALK* was also detected in both cell lines.

Sensitivity of the Assay

The major variant forms of *EML4-ALK* are variants 1, 3a, and 3b, which account for ~60% of all *EML4-ALK* fusions.[7]

TABLE 1. Characteristics of Patients Screened for *EML4-ALK*

No.	Age (years)	Sex	Histology	Procedure	Smoking status	*EML4-ALK*
1	63	F	Ad	TLB	Never	Negative
2	62	M	Ad	TBLB	Current	Negative
3	74	M	Ad	TLB	Current	Negative
4	71	M	Ad	TBLB	Current	Negative
5	63	F	Ad	TBLB	Never	Variant 1
6	75	M	Ad	TBLB	Former	Negative
7	59	M	Ad	Needle biopsy	Current	Negative
8	85	M	Ad	TBLB	Current	Negative
9	73	F	Ad	Lymph node biopsy	Never	Negative
10	68	F	Ad	TBLB	Current	Negative
11	65	M	Ad	TBLB	Current	Variant 1
12	57	M	Ad	TBLB	Current	Negative
13	68	F	Ad	TLB	Never	Negative
14	73	M	Ad	TBLB	Former	Negative
15	67	F	Ad	TBLB	Never	Negative
16	67	M	Ad	TBLB	Former	Negative
17	57	M	Ad	TBLB	Former	Negative
18	56	M	Large	TBLB	Current	Negative
19	65	M	Ad	TBLB	Current	Negative
20	60	M	Ad	TBLB	Current	Variant 1

Ad, adenocarcinoma; Large, large cell carcinoma; TLB, thoracoscopic lung biopsy; TBLB, transbronchial lung biopsy.

We therefore examined the sensitivity of our assay for detection of these variants. Samples containing 1000, 100, 10, or 1 copy of plasmid DNA [pcDNA3.1(+) for variants 1, 3a, or 3b] and 1 ng of normal human genomic DNA (Promega, Madison, WI) were prepared by 10-fold serial dilution. MS spectra revealed a clear peak at the expected size for variants 1, 3a, or 3b in all samples, including those containing only one copy of the variant DNA (Fig. 3*A*). We also examined assay sensitivity when the samples were diluted with pCR2.1 containing *ALK* cDNA (pCR2.1-alk). Samples containing 1000, 100, 10, or 1 copy of the variant plasmids were thus diluted with 10 pg (~2 × 10^6 copies) of pCR2.1-alk. A clear peak at the expected size was again detected in all the samples including those containing only one copy of the variant DNA (Fig. 3*B*). These results therefore suggested that the sensitivity of the assay for the detection of *EML4-ALK* variants is high.

Detection of *EML4-ALK* Variants in FFPE Samples

We next evaluated the ability of our assay to detect *EML4-ALK* variants in three surgically resected FFPE samples of NSCLC shown to be positive for *ALK* rearrangements by FISH analysis (Fig. 4*A*). The primary PCR products for the assay were also analyzed by gel electrophoresis, with the expected sizes of the amplification products being 115, 103, and 119 bp for variants 1, 3a, and 3b, respectively. Bands corresponding to *EML4-ALK* variant 1 (case 2), variant 3a (cases 1 and 3), and variant 3b (case 3) were detected (Fig. 4*B*). Similarly, we detected MS peaks corresponding to *EML4-ALK* variant 1 and to variants 3a or 3b in case 2 and in cases 1 and 3, respectively (Fig. 4*C*). The presence of *EML4-ALK* variants in these three cases was confirmed by subcloning and sequencing of PCR products (Fig. 4*D*). We further analyzed several NSCLC specimens shown to be negative for *EML4-ALK* by FISH analysis; no mass peaks for *EML4-ALK* variants were detected by the MassARRAY assay (data not shown). These results thus suggested that the MassARRAY assay is able to detect *EML4-ALK* variants in FFPE samples.

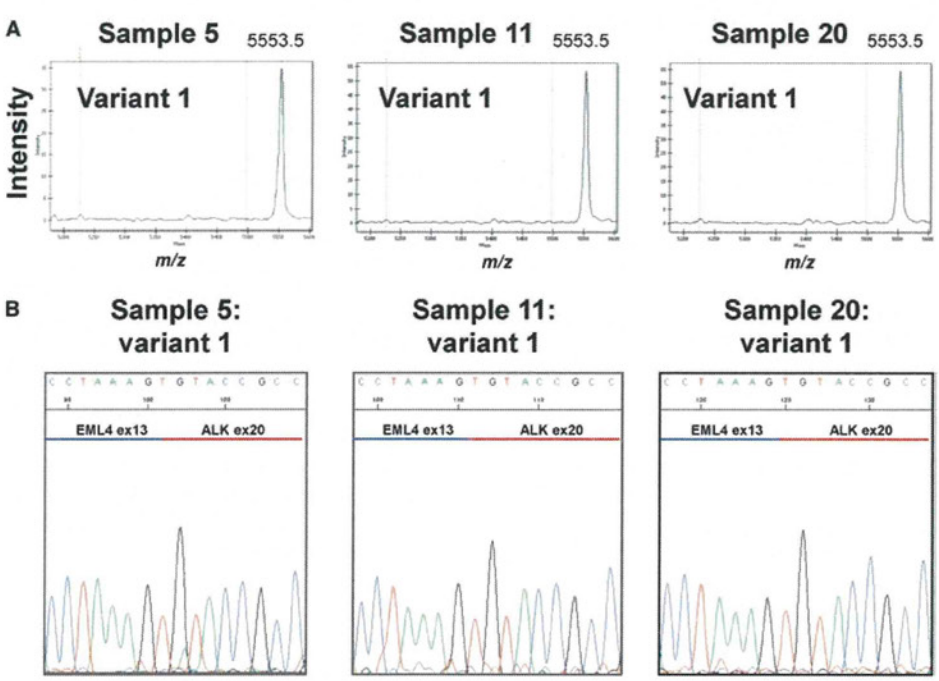

FIGURE 5. Detection of *EML4-ALK* in formalin-fixed, paraffin-embedded samples of non–small cell lung cancer obtained by transbronchial lung biopsy. (*A*) Representative spectra of *EML4-ALK*–positive samples. The experiments were repeated twice with identical results. (*B*) The polymerase chain reaction products from (*A*) were subcloned and sequenced.

Screening for *EML4-ALK* Variants in FFPE Biopsy Samples of Advanced NSCLC

Molecular analysis of biopsy samples from patients with advanced NSCLC is often difficult because of the small amount of tissue available. We therefore examined the feasibility of detection of *EML4-ALK* variants with the MassARRAY assay in FFPE biopsy specimens obtained from 20 patients with advanced NSCLC, the characteristics of whom are shown in Table 1. Three specimens (samples 5, 11, and 20) were found to be positive for variant 1 of *EML4-ALK*, with none of the other variants being detected (Fig. 5*A*). The presence of *EML4-ALK* variant 1 in these three cases was confirmed by subcloning and sequencing of PCR products (Fig. 5*B*). We also performed FISH analysis on the 20 FFPE specimens. Of the three *EML4-ALK*–positive cases detected by the MassARRAY assay, two (samples 5 and 20) were positive by FISH whereas the third (sample 11) could not be evaluated because of poor tissue quality (data not shown). None of the cases that tested negative by the MassARRAY assay was positive by FISH. These results thus suggested that our assay is effective for *EML4-ALK* screening with FFPE biopsy specimens of advanced NSCLC.

DISCUSSION

We have developed a MassARRAY assay for screening of *EML4-ALK* in FFPE samples of NSCLC tissue. This novel assay is capable of detecting nine different *EML4-ALK* variants with a high sensitivity.

Dual-color split-signal FISH analysis has been considered the gold standard in screening for *ALK* rearrangement. However, given that *EML4* and *ALK* loci are located in relatively close proximity on chromosome 2p, the detection of the *EML4-ALK* fusion gene on the basis of the gap between the probes is sometimes difficult. The identification and counting of signals on tissue sections is impeded by factors such as cutting artifacts and nuclear overlap related to the thickness and homogeneity of the tissue sections and the size of the nuclei. The MassARRAY system is a nucleic acid analysis platform which utilizes a three-step process composed of PCR amplification, single-base primer extension, and MALDI–TOF MS analysis. The presence of *EML4-ALK* in our MassARRAY assay is detected on the basis of the presence of products of predicted mass.

The amount of tumor tissue available for molecular analysis is often limited in patients with advanced NSCLC. Furthermore, RNA extracted from FFPE samples is highly degraded and less amenable to RT-PCR analysis compared with that isolated from nonfixed, freshly frozen tissue. We succeeded in amplifying *EML4-ALK* cDNA by PCR from FFPE tissue with primers designed to yield short amplicons (70–130 bp). The design of such short amplicons can also be applied to quantitative PCR systems such as amplification-refractory mutation system for allele-specific PCR assays. In our system, PCR amplification was performed with a high number of cycles (45 cycles), and increased accumulation of PCR products conferred higher sensitivity. We tested 20 FFPE biopsy samples from patients with NSCLC with our assay and detected a clear mass peak for *EML4-ALK* variant 1 in 3 of these samples, each of which was confirmed positive for this variant by subcloning and sequencing of the PCR products. In contrast to FISH, our assay is able to distinguish between the different *EML4-ALK* variants in a small amount of FFPE NSCLC tissue, and it should prove to be a useful tool for the detection of *EML4-ALK* variants in diagnostic testing for this fusion gene.

ACKNOWLEDGMENTS

Supported by the Third-Term Comprehensive 10-Year Strategy for Cancer Control of the Ministry of Education, Culture, Sports, Science, and Technology of Japan as well as by Health and Labor Scientific Research Grants [20-9].

REFERENCES

1. Soda M, Choi YL, Enomoto M, et al. Identification of the transforming EML4-ALK fusion gene in non-small-cell lung cancer. *Nature* 2007;448:561–566.
2. Takeuchi K, Choi YL, Soda M, et al. Multiplex reverse transcription-PCR screening for EML4-ALK fusion transcripts. *Clin Cancer Res* 2008;14:6618–6624.
3. Choi YL, Takeuchi K, Soda M, et al. Identification of novel isoforms of the EML4-ALK transforming gene in non-small cell lung cancer. *Cancer Res* 2008;68:4971–4976.
4. Takeuchi K, Choi YL, Togashi Y, et al. KIF5B-ALK, a novel fusion oncokinase identified by an immunohistochemistry-based diagnostic system for ALK-positive lung cancer. *Clin Cancer Res* 2009;15:3143–3149.
5. Sasaki T, Rodig SJ, Chirieac LR, Jänne PA. The biology and treatment of EML4-ALK non-small cell lung cancer. *Eur J Cancer* 2010;46:1773–1780.
6. Kwak EL, Bang YJ, Camidge DR, et al. Anaplastic lymphoma kinase inhibition in non-small-cell lung cancer. *N Engl J Med* 2010;363:1693–1703.
7. Koivunen JP, Mermel C, Zejnullahu K, et al. EML4-ALK fusion gene and efficacy of an ALK kinase inhibitor in lung cancer. *Clin Cancer Res* 2008;14:4275–4283.
8. Inamura K, Takeuchi K, Togashi Y, et al. EML4-ALK fusion is linked to histological characteristics in a subset of lung cancers. *J Thorac Oncol* 2008;3:13–17.
9. Wong DW, Leung EL, So KK, et al.; University of Hong Kong Lung Cancer Study Group. The EML4-ALK fusion gene is involved in various histologic types of lung cancers from nonsmokers with wild-type EGFR and KRAS. *Cancer* 2009;115:1723–1733.
10. Martelli MP, Sozzi G, Hernandez L, et al. EML4-ALK rearrangement in non-small cell lung cancer and non-tumor lung tissues. *Am J Pathol* 2009;174:661–670.
11. Rodig SJ, Mino-Kenudson M, Dacic S, et al. Unique clinicopathologic features characterize ALK-rearranged lung adenocarcinoma in the western population. *Clin Cancer Res* 2009;15:5216–5223.
12. Takezawa K, Okamoto I, Nishio K, Jänne PA, Nakagawa K. Role of ERK-BIM and STAT3-survivin signaling pathways in ALK inhibitor-induced apoptosis in EML4-ALK-positive lung cancer. *Clin Cancer Res* 2011;17:2140–2148.

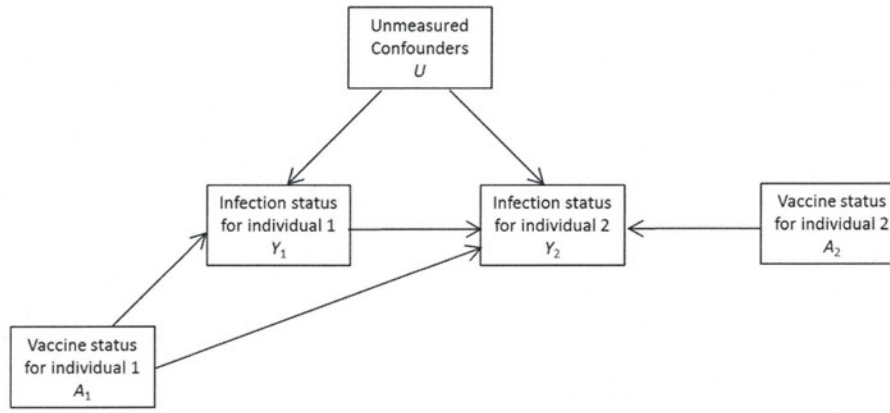

Fig. 1. A directed acyclic graph for a setting of this paper with vaccine status for individual j (A_j), infection status for individual j (Y_j), and a set of unmeasured confounders (U).

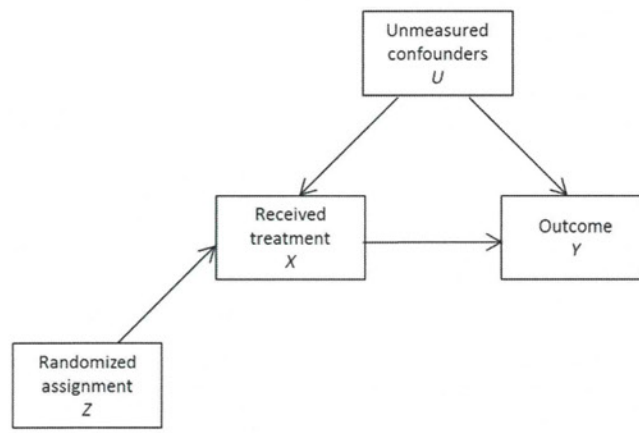

Fig. 2. A directed acyclic graph for a setting of the CACE paper with randomized assignment (Z), received treatment (X), an outcome (Y), and a set of unmeasured confounders (U).

effect of A_1 and A_2 on Y_2 in a principal stratum, while the CACE focuses on the causal effect of X on Y in the other principal stratum. Because of these differences, the mathematical results in the two papers are different, and we cannot deduce one from the other.

2. Notation and definitions

Following VanderWeele and Tchetgen Tchetgen (2011), we consider a setting in which there are N households, indexed by $i = 1, \ldots, N$, in which each household consists of two persons, indexed by $j = 1, 2$. Let A_{ij} denote the vaccine status for individual j in household i ($A_{ij} = 1$ if the individual received the vaccination, and $A_{ij} = 0$ if otherwise). For each household, let $A_i = (A_{i1}, A_{i2})$ denote the vaccine status of the two individuals in the household. Let Y_{ij} denote the infection status of individual j in household i after some suitable follow-up in the study ($Y_{ij} = 1$ if infected, and $Y_{ij} = 0$ if uninfected). Let $Y_{ij}(a_1, a_2)$ denote the counterfactual outcome for individual j in household i if the two individuals in household i had, possibly contrary to fact, vaccine status (a_1, a_2). Note that $Y_{ij}(a_1, a_2)$ depends on the vaccine status of both individual 1 and individual 2. This allows for the possibility that the vaccine status of one person affects the outcome of another, which is sometimes referred to as interference. However, we assume that the vaccine status of persons in one household in the study does not affect the outcomes of those in other study households, which is sometimes referred to as partial interference (Sobel, 2006; Hudgens and Halloran, 2008).

We assume a randomized trial in which one of the two persons is randomized to receive a vaccine or control, and the second person is always unvaccinated. We further require the consistency assumption that $Y_{ij}(A_1, A_2) = Y_{ij}$ for all individuals, so that the value of Y that would have been observed if $A = (A_1, A_2)$ had been set to what it in fact was, is equal to the value of Y that was in fact observed. This assumption implies that $E[Y_{ij}(a_1, a_2) \mid A_{i1} = a_1, A_{i2} = a_2] = E[Y_{ij} \mid A_{i1} = a_1, A_{i2} = a_2]$, where E denotes the expectation taken over households i, assuming a random sample of households from a larger super-population of households.

The crude estimator for the infectiousness effect might be taken as

$$E[Y_{i2} \mid A_{i1} = 1, Y_{i1} = 1] - E[Y_{i2} \mid A_{i1} = 0, Y_{i1} = 1].$$

This compares the infection status for individual 2 in the subgroup in which individual 1 was vaccinated and infected versus that in the subgroup in which individual 1 was unvaccinated and infected. Although the vaccine status for individual 1, A_{i1}, is randomized, conditioning on a variable that occurs after treatment breaks randomization (Rosenbaum, 1984; Pearl, 2009). Therefore, the crude estimator may not make a fair comparison, because the subgroup in which individual 1 is vaccinated and infected may be quite different from that in which individual 1 is unvaccinated and infected. To avoid this problem, the CIE is defined as

$$\text{CIE} \equiv E_{11}(1, 0) - E_{11}(0, 0)$$

where $E_{kl}(a_1, a_2) \equiv E[Y_{i2}(a_1, a_2) \mid Y_{i1}(1, 0) = k, Y_{i1}(0, 0) = l]$ (Hudgens and Halloran, 2006; Tchetgen Tchetgen and VanderWeele, 2012). This compares the infection status for individual 2 if individual 1 was vaccinated, $Y_{i2}(1, 0)$, versus unvaccinated, $Y_{i2}(0, 0)$, among the subset of households for whom individual 1 would have been infected irrespective of whether individual 1 was vaccinated, *i.e.*, $Y_{i1}(1, 0) = Y_{i1}(0, 0) = 1$. Such a subgroup is sometimes referred to as the principal stratum (Frangakis and Rubin, 2002; Rubin, 2004).

Note that the vaccination of individual 1 may prevent individual 2 from being infected via two mechanisms: (i) the vaccine may prevent individual 1 from acquiring the infection and thereby reduce the probability of transmission to individual 2 or (ii) if individual 1 is infected irrespective of the vaccine, the vaccine may impair the ability of the infectious agent to initiate new infections, *i.e.*, make the agent less infectious. Only the latter mechanism is included under the CIE.

3. Bounds for the causal infectiousness effect

We define the sensitivity parameter, which is used to derive the CIE bounds, as follows:

$$\alpha_y \equiv E[Y_{i2}(0, 0) \mid A_{i1} = 1, Y_{i1} = y] - E[Y_{i2}(0, 0) \mid A_{i1} = 0, Y_{i1} = y],$$

where $y = 0, 1$, which is an extension of a sensitivity parameter developed in the context of causal mediation analysis (Chiba, 2010; Chiba and VanderWeele, 2011) to the CIE. α_y compares two subgroups: (i) the subgroup of households for which individual 1 was actually vaccinated and (ii) the subgroup of households for which individual 1 was actually unvaccinated, where the infection status is equal among these two subgroups.

To derive the CIE bounds, we require two assumptions. The first assumption states that the vaccine will never be the cause of the infection; *i.e.*, there may be doomed households who would be infected irrespective of vaccination status ($Y_{i1}(1, 0) = Y_{i1}(0, 0) = 1$), immune households who would not be infected irrespective of vaccination status ($Y_{i1}(1, 0) = Y_{i1}(0, 0) = 0$), or causative households who would be infected if unvaccinated and not infected if vaccinated ($Y_{i1}(1, 0) = 0$ and $Y_{i1}(0, 0) = 1$), but there is no preventive household who would be infected if vaccinated but uninfected if unvaccinated ($Y_{i1}(1, 0) = 1$ and $Y_{i1}(0, 0) = 0$). This assumption is sometimes referred to as a monotonicity assumption (Angrist et al., 1996; Dawid, 2000), and it is formalized as follows in the vaccine trial (VanderWeele and Tchetgen Tchetgen, 2011):

Assumption 1. $Y_{i1}(1, 0) \leq Y_{i1}(0, 0)$ for all i.

Using α_y, under Assumption 1, the CIE can be expressed as

$$\text{CIE} = P_{11} - P_{01} - \alpha_1 \tag{1}$$

where $P_{ay} = E[Y_{i2} \mid A_{i1} = a, Y_{i1} = y]$, and the relationship between α_0 and α_1 is as follows:

$$\alpha_1 = \frac{(p_0 - p_1)(P_{01} - P_{00}) - (1 - p_1)\alpha_0}{p_1}, \tag{2}$$

where $p_a = \Pr(Y_{i1} = 1 \mid A_{i1} = a)$. The derivations are given in Appendix A. (1) shows that we can conduct a sensitivity analysis for the CIE using the sensitivity parameter α_1.

The second assumption states that the probability of infection for individual 2 if both individuals 1 and 2 were unvaccinated would be lower in the subgroup of households for which individual 1 was unvaccinated and uninfected than in that for which individual 1 was vaccinated and uninfected. In addition, it would be lower in the subgroup of households for which individual 1 was unvaccinated and infected than in that for which individual 1 was vaccinated and infected. This can be formalized as follows:

Assumption 2. $\alpha_y \geq 0$ for $y = 0, 1$.

This assumption is equivalent to $E[Y_{i2}(0,0) \mid A_{i1} = 1, Y_{i1} = y] \geq E[Y_{i2}(0,0) \mid A_{i1} = 0, Y_{i1} = y]$, which is arguably reasonable insofar as the subgroup for which individual 1 was vaccinated is likely to be less healthy (or the infection is more virulent) than the subgroup for which individual 1 was unvaccinated; thus, under the scenario in which both people are unvaccinated, individual 2 is more likely to be infected in the first group than in the second group. If this is indeed the case, Assumption 2 will hold.

Under Assumption 1, Assumption 2 is equivalent to assuming that

$$E_{11}(0,0) \geq E_{01}(0,0) \tag{3}$$

with $y = 1$, and

$$E_{01}(0,0) \geq E_{00}(0,0) \tag{4}$$

with $y = 0$. The proof is given in Appendix B. (3) implies that the probability of infection for individual 2 in the doomed households is not less than that in the causative households, and (4) implies that the probability of infection for individual 2 in the causative households is not less than that in the immune households. This observation shows that Assumption 2 is arguably reasonable in many actual vaccine trials when Assumption 1 holds, because the probability of infection for individual 2 in the doomed households would be the highest and that in the immune households would be the lowest of the three principal strata, excluding the preventive households.

Under Assumptions 1 and 2, (2) gives

$$0 \leq \alpha_1 \leq \frac{(p_0 - p_1)(P_{01} - P_{00})}{p_1}. \tag{5}$$

Note that, when Assumption 1 holds, $p_0 > p_1$ if there is at least one causative household, and $P_{01} \geq P_{00}$ under Assumption 2 (see Appendix A). Therefore, we can say that Assumption 2 does not hold if the observed data show that $P_{01} < P_{00}$, when Assumption 1 holds.

We obtain the following result by substituting (5) into (1):

Result 1. Under Assumptions 1 and 2,

$$\frac{P_{1\bullet} - P_{0\bullet} - (1 - p_1)(P_{10} - P_{00})}{p_1} \leq \mathrm{CIE} \leq P_{11} - P_{01},$$

where $P_{a\bullet} = E[Y_{i2} \mid A_{i1} = a]$.

Note that VanderWeele and Tchetgen Tchetgen (2011) showed that $\mathrm{CIE} \leq P_{11} - P_{01}$ under Assumption 1 and $\alpha_1 \geq 0$ (*i.e.*, Assumption 2 with $y = 1$). Therefore, Result 1 implies that we can derive both bounds for the CIE under slightly stronger assumptions than theirs.

4. Discussion

We have presented both bounds for the CIE under two plausible assumptions that may be reasonable in many vaccine trials as mentioned in the section above, whereas VanderWeele and Tchetgen Tchetgen (2011) derived the upper bound under slightly weaker assumptions. The bounds presented here are based on estimated quantities. Some researchers may be interested in confidence intervals (CIs) of the bounds; they can be derived from both bounds of Result 1, although the CI formula of the lower bound may be somewhat complex. We can also employ a sensitivity analysis method by using (1), where fixed values of α_1 are examined within a range of (5). Then, to obtain the CI for the CIE for a fixed value of α_1, one can simply subtract α_1 from the upper and lower confidence limits for $P_{11} - P_{01}$.

Result 1 was obtained by applying the idea developed in the context of causal mediation analysis. This implies that if the sample is large, we will be able to derive the large sample bounds (Zhang and Rubin, 2003; Zhang et al., 2008; Halloran and Hudgens, 2012; Chiba, in press), even for cases in which only Assumption 1 holds or neither Assumption 1 nor 2 holds, although the bounds may be somewhat broad. The lower bound under Assumptions 1 and 2 with $y = 1$ can be also derived using the large sample bounds (see Appendix C for the details).

In this paper, we defined the CIE on a risk-difference scale. We can extend the result presented here to other measures of the effect straightforwardly because $E_{11}(1,0) = P_{11}$ and $E_{11}(0,0) = P_{01} + \alpha_1$ under Assumption 1 (see Appendix A). For example, on a risk-ratio scale, $E_{11}(1,0)/E_{11}(0,0) = P_{11}/(P_{01} + \alpha_1)$, and the bounds can be derived by substituting (3) into this equation.

VanderWeele and Tchetgen Tchetgen (2011) also discussed the case with selection bias due to competing pathogen strength and the case in which both individuals are randomized. They showed that the upper bound for the CIE becomes the crude estimator even in these cases, with an additional assumption for the former case. Our result can also be extended to the latter case straightforwardly. The results are given in Appendix D. However, it may be difficult to extend our result to the former case. For this case, VanderWeele and Tchetgen Tchetgen (2011) defined pathogen-virulence conditional infectiousness effects as

$$E[Y_{i2}(1,0) - Y_{i2}(0,0) \mid Y_{i1}(1,0) = Y_{i1}(0,0) = 1, S_i(1) = S_i(0) = s],$$

where $S_i(0)$ and $S_i(1)$ are the virulence of the pathogen causing the infection when individual 1 was unvaccinated and vaccinated, respectively. In this case, the derivation of the lower bound for CIE will be very complex, because we must consider four sensitivity parameters for $y = 0, 1$ and $s = 0, 1$ instead of two sensitivity parameters of α_0 and α_1. Further research is needed for this case.

Acknowledgments

This work was supported partially by Grant-in-Aid for Scientific Research (No. 23700344) from the Ministry of Education, Culture, Sports, Science, and Technology of Japan. The author thanks the reviewers for their helpful comments.

Appendix A. Derivations of (1) and (2)

Here, we use the notation $\pi_{kl} \equiv \Pr(Y_{i1}(1, 0) = k, Y_{i1}(0, 0) = l)$. The relationships between π_{kl} and p_a are then

$$\pi_{10} + \pi_{11} = p_1, \quad \pi_{00} + \pi_{01} = 1 - p_1, \quad \pi_{11} + \pi_{01} = p_0, \quad \text{and} \quad \pi_{10} + \pi_{00} = 1 - p_0, \tag{A.1}$$

because $\Pr(Y_{i1}(a_1, 0) = y_1) = \Pr(Y_{i1}(a_1, 0) = y_1 \mid A_{i1} = a_1) = \Pr(Y_{i1} = y_1 \mid A_{i1} = a_1)$ by randomization and the consistency assumption. Furthermore, because individuals in the subgroup with $(A_{i1}, Y_{i1}) = (1, 1)$ must be either doomed or preventive households (immune or causative households cannot take a paired observation of $(A_{i1}, Y_{i1}) = (1, 1)$), the following equation holds:

$$E[Y_{i2}(a_1, 0) \mid A_{i1} = 1, Y_{i1} = 1] = \frac{\pi_{11}E_{11}(a_1, 0) + \pi_{10}E_{10}(a_1, 0)}{\pi_{11} + \pi_{10}}. \tag{A.2}$$

Similarly,

$$E[Y_{i2}(a_1, 0) \mid A_{i1} = 1, Y_{i1} = 0] = \frac{\pi_{01}E_{01}(a_1, 0) + \pi_{00}E_{00}(a_1, 0)}{\pi_{01} + \pi_{00}}, \tag{A.3}$$

$$E[Y_{i2}(a_1, 0) \mid A_{i1} = 0, Y_{i1} = 1] = \frac{\pi_{11}E_{11}(a_1, 0) + \pi_{01}E_{01}(a_1, 0)}{\pi_{11} + \pi_{01}}, \tag{A.4}$$

$$E[Y_{i2}(a_1, 0) \mid A_{i1} = 0, Y_{i1} = 0] = \frac{\pi_{10}E_{10}(a_1, 0) + \pi_{00}E_{00}(a_1, 0)}{\pi_{10} + \pi_{00}}. \tag{A.5}$$

As $\pi_{10} = 0$ (there is no preventive household) under Assumption 1, (A.1) reduces to

$$\pi_{11} = p_1, \quad \pi_{00} = 1 - p_0, \quad \text{and} \quad \pi_{01} = p_0 - p_1,$$

where it is assumed that $\pi_{01} > 0$ (*i.e.*, $p_0 > p_1$), which implies that there is at least one causative household. (A.2)–(A.5) can then be expressed as

$$E[Y_{i2}(a_1, 0) \mid A_{i1} = 1, Y_{i1} = 1] = E_{11}(a_1, 0), \tag{A.6}$$

$$E[Y_{i2}(a_1, 0) \mid A_{i1} = 1, Y_{i1} = 0] = \frac{(p_0 - p_1)E_{01}(a_1, 0) + (1 - p_0)E_{00}(a_1, 0)}{1 - p_1}, \tag{A.7}$$

$$E[Y_{i2}(a_1, 0) \mid A_{i1} = 0, Y_{i1} = 1] = \frac{p_1E_{11}(a_1, 0) + (p_0 - p_1)E_{01}(a_1, 0)}{p_0}, \tag{A.8}$$

$$E[Y_{i2}(a_1, 0) \mid A_{i1} = 0, Y_{i1} = 0] = E_{00}(a_1, 0), \tag{A.9}$$

respectively.

(A.6) with $a_1 = 1$ yields

$$\begin{aligned} E_{11}(1, 0) &= E[Y_{i2}(1, 0) \mid A_{i1} = 1, Y_{i1} = 1] \\ &= P_{11}, \end{aligned}$$

and using $\alpha_1 = E[Y_{i2}(0, 0) \mid A_{i1} = 1, Y_{i1} = 1] - P_{01}$, with $a_1 = 0$, it yields

$$\begin{aligned} E_{11}(0, 0) &= E[Y_{i2}(0, 0) \mid A_{i1} = 1, Y_{i1} = 1] \\ &= P_{01} + \alpha_1. \end{aligned}$$

The difference between them is (1).

By substituting the above equation into (A.8) with $a_1 = 0$, we have

$$\begin{aligned} E_{01}(0,0) &= \frac{p_0 E[Y_{i2}(0,0) \mid A_{i1}=0, Y_{i1}=1] - p_1 E_{11}(0,0)}{p_0 - p_1} \\ &= \frac{p_0 P_{01} - p_1(P_{01}+\alpha_1)}{p_0 - p_1} \\ &= P_{01} - \frac{p_1}{p_0 - p_1}\alpha_1. \end{aligned}$$

Likewise, by substituting (A.9) into (A.7) with $a_1 = 0$ and using $\alpha_0 = E[Y_{i2}(0,0) \mid A_{i1}=1, Y_{i1}=0] - P_{00}$, we have

$$\begin{aligned} E_{01}(0,0) &= \frac{(1-p_1)E[Y_{i2}(0,0) \mid A_{i1}=1, Y_{i1}=0] - (1-p_0)E_{00}(0,0)}{p_0 - p_1} \\ &= \frac{(1-p_1)(P_{00}+\alpha_0) - (1-p_0)P_{00}}{p_0 - p_1} \\ &= P_{00} + \frac{1-p_1}{p_0 - p_1}\alpha_0. \end{aligned}$$

Given that these two equations are equal, some algebra yields (2). Furthermore, under Assumption 2, these two equations yield $P_{00} \le E_{01}(0,0) \le P_{01}$, *i.e.*, $P_{00} \le P_{01}$.

Appendix B. Proof that Assumption 2 is equivalent to (3) and (4) under Assumption 1

Under Assumption 1, (A.6)–(A.9) hold. Under Assumption 2 with $y = 1$, (A.6) and (A.8) lead to

$$\begin{aligned} &E[Y_{i2}(0,0) \mid A_{i1}=1, Y_{i1}=1] \ge E[Y_{i2}(0,0) \mid A_{i1}=0, Y_{i1}=1] \\ &\Leftrightarrow (p_0 - p_1)E_{11}(0,0) \ge (p_0 - p_1)E_{01}(0,0), \end{aligned}$$

and under Assumption 2 with $y = 0$, (A.7) and (A.9) lead to

$$\begin{aligned} &E[Y_{i2}(0,0) \mid A_{i1}=1, Y_{i1}=0] \ge E[Y_{i2}(0,0) \mid A_{i1}=0, Y_{i1}=0] \\ &\Leftrightarrow (p_0 - p_1)E_{01}(0,0) \ge (p_0 - p_1)E_{00}(0,0). \end{aligned}$$

This completes the proof because $p_0 > p_1$ by assumption.

Appendix C. Large sample bounds

The large sample bounds are derived from the numbers of doomed households ($Y_{i1}(1,0) = Y_{i1}(0,0) = 1$) in households assigned to $A_{i1} = 0, 1$. With no assumption, $\pi_{11} \ge \max\{0, p_0 + p_1 - 1\}$ because $\pi_{11} = 1 - p_0 - p_1 + \pi_{00}$ from (A.1) and $0 \le \pi_{kl} \le 1$. As mentioned in Appendix A, households in the subgroup with $(A_{i1}, Y_{i1}) = (1,1)$ must be either doomed or preventive households. Thus, if $p_0 + p_1 - 1 > 0$, the proportion of doomed households in this subgroup is $\pi_{11}/(\pi_{11} + \pi_{10}) = \pi_{11}/p_1$ from (A.1), and the number must be $N_{11}\pi_{11}/(\pi_{11} + \pi_{10}) \ge N_{11}(p_0 + p_1 - 1)/p_1$, where N_{a1} denotes the number of households with $(A_{i1}, Y_{i1}) = (a, 1)$. Applying this lower bound, the lower bound of $E_{11}(1,0)$ is the expectation if $N_{11}(p_0 + p_1 - 1)/p_1$ of households in the subgroup with $(A_{i1}, Y_{i1}) = (1,1)$ take the smallest values of Y_{i2} in sequence, and the upper bound of $E_{11}(1,0)$ is the expectation if the number of households take the largest values of Y_{i2} in sequence.

Likewise, in the subgroup with $(A_{i1}, Y_{i1}) = (0,1)$, the proportion of doomed households is $\pi_{11}/(\pi_{11}+\pi_{01}) = \pi_{11}/p_0$, and thus the number must be $N_{01}\pi_{11}/(\pi_{11} + \pi_{01}) \ge N_{01}(p_0 + p_1 - 1)/p_0$. The lower bound of $E_{11}(0,0)$ is then the expectation if $N_{01}(p_0 + p_1 - 1)/p_0$ of households in the subgroup with $(A_{i1}, Y_{i1}) = (0,1)$ take the smallest values of Y_{i2} in sequence, and the upper bound of $E_{11}(0,0)$ is the expectation if the number of households take the largest values of Y_{i2} in sequence.

For example, consider the hypothetical data set of Table 1. As $N_{01}(p_0 + p_1 - 1)/p_1 = N_{01}(p_0 + p_1 - 1)/p_0 = 400$, the large sample bounds of $E_{11}(a_1, 0)$ are calculated by

$$\begin{aligned} \frac{0 \times 300 + 1 \times (400 - 300)}{400} &\le E_{11}(1,0) \le \frac{1 \times 300 + 0 \times (400 - 300)}{400}, \\ \frac{0 \times 320 + 1 \times (400 - 320)}{400} &\le E_{11}(0,0) \le \frac{1 \times 400 + 0 \times (400 - 400)}{400}. \end{aligned}$$

These bounds lead to the CIE bounds of $-0.75 \le \text{CIE} \le 0.55$.

Under Assumption 1, $E_{11}(1,0) = P_{11} = 0.50$ and $\pi_{11} = p_1$ as shown in Appendix A. Then, the number of doomed households in the subgroup with $(A_{i1}, Y_{i1}) = (0,1)$ is $N_{01}\pi_{11}/(\pi_{11} + \pi_{01}) = N_{01}p_1/p_0 = 600$, and thus the large sample bounds of $E_{11}(0,0)$ are

$$\frac{0 \times 320 + 1 \times (600 - 320)}{600} \le E_{11}(0,0) \le \frac{1 \times 480 + 0 \times (600 - 480)}{600}.$$

Table 1
Hypothetical data set.

	$A_1 = 1$		$A_1 = 0$	
	$Y_1 = 1$	$Y_1 = 0$	$Y_1 = 1$	$Y_1 = 0$
$Y_2 = 1$	300	40	480	60
$Y_2 = 0$	300	360	320	140
Total	600	400	800	200

Therefore, the large sample bounds for the CIE become $-0.30 \leq \text{CIE} \leq 0.03$. Note that the upper bound is improved to -0.10 by adding Assumption 2 with $y = 1$, and the lower bound is improved to -0.20 by the further addition of Assumption 2 with $y = 0$.

Appendix D. Case in which both individuals are randomized

Here, we discuss the case in which both of the two individuals are randomized to receive the vaccine or control. In addition to

$$\text{CIE} \equiv E[Y_{i2}(1,0) - Y_{i2}(0,0) \mid Y_{i1}(1,0) = Y_{i1}(0,0) = 1]$$

defined in the manuscript, we could also define a further CIE of

$$\text{CIE} \equiv E[Y_{i1}(1,1) - Y_{i1}(1,0) \mid Y_{i2}(1,1) = Y_{i2}(1,0) = 1].$$

Using the notation

$$E_{2,kl}(a_1, a_2) \equiv E[Y_{i2}(a_1, a_2) \mid Y_{i1}(1,0) = k, Y_{i1}(0,0) = l],$$
$$E_{1,kl}(a_1, a_2) \equiv E[Y_{i1}(a_1, a_2) \mid Y_{i2}(1,1) = k, Y_{i2}(1,0) = l],$$

we rewrite these CIEs as follows:

$$\text{CIE}_2 \equiv E_{2,11}(1,0) - E_{2,11}(0,0),$$
$$\text{CIE}_1 \equiv E_{1,11}(1,1) - E_{1,11}(1,0).$$

Furthermore, we use the notation

$$p_{j,ab} \equiv \Pr(Y_{ij} = 1 \mid A_{i1} = a, A_{i2} = b),$$
$$\beta_{2y} \equiv E[Y_{i2}(0,0) \mid A_{i1} = 1, A_{i2} = 0, Y_{i1} = y] - E[Y_{i2}(0,0) \mid A_{i1} = 0, A_{i2} = 0, Y_{i1} = y],$$
$$\beta_{1y} \equiv E[Y_{i1}(1,0) \mid A_{i1} = 1, A_{i2} = 1, Y_{i2} = y] - E[Y_{i1}(1,0) \mid A_{i1} = 1, A_{i2} = 0, Y_{i2} = y],$$

where β_{2y} and β_{1y} are sensitivity parameters instead of α_y in the manuscript.

First, we present the bounds for CIE_2 under Assumption 1 and a modification of Assumption 2. The modified assumption is as follows:

Assumption 2^*. $\beta_{2y} \geq 0$ for $y = 0, 1$.

This assumption is explicitly conditional on $A_{i2} = 0$ in Assumption 2. Therefore, the bounds for CIE_2 simply become those of Result 1 conditional on $A_{i2} = 0$; *i.e.*, under Assumption 1,

$$\text{CIE}_2 = P_{2,101} - P_{2,001} - \beta_{21},$$

where $P_{2,aby} = E[Y_{i2} \mid A_{i1} = a, A_{i2} = b, Y_{i1} = y]$, and

$$\beta_{21} = \frac{(p_{1,00} - p_{1,10})(P_{2,001} - P_{2,000}) - (1 - p_{1,10})\beta_{20}}{p_{1,10}},$$

instead of (1) and (2) in the manuscript, and we have the following result:

Result 2. Under Assumptions 1 and 2^*,

$$\frac{P_{2,10\bullet} - P_{2,00\bullet} - (1 - p_{1,10})(P_{2,100} - P_{2,000})}{p_{1,10}} \leq \text{CIE}_2 \leq P_{2,101} - P_{2,001},$$

where $P_{2,ab\bullet} = E[Y_{i2} \mid A_{i1} = a, A_{i2} = b]$.

Second, we present the bounds for CIE_1 with modifications of Assumptions 1 and 2. The modified assumptions are as follows:

Assumption 1^*. $Y_{i2}(1,1) \leq Y_{i2}(1,0)$ for all i.

Assumption 2^{**}. $\beta_{1y} \geq 0$ for $y = 0, 1$.

Result 3. Under Assumptions 1^* and 2^{**},

$$\frac{P_{1,10\bullet} - P_{1,00\bullet} - (1 - p_{2,10})(P_{1,110} - P_{1,100})}{p_{2,10}} \leq \mathrm{CIE}_1 \leq P_{1,111} - P_{1,101},$$

where $P_{1,aby} = E[Y_{i1} \mid A_{i1} = a, A_{i2} = b, Y_{i2} = y]$ and $P_{1,ab\bullet} = E[Y_{i1} \mid A_{i1} = a, A_{i2} = b]$.

This result is obtained by replacing individual 1 with individual 2, along with the replacement of $Y_{i2}(a_1, 0)$ with $Y_{i1}(1, a_2)$.

Note that VanderWeele and Tchetgen Tchetgen (2011) showed that $\mathrm{CIE}_2 \leq P_{2,101} - P_{2,001}$ under Assumption 1 and $\beta_{21} \geq 0$ (*i.e.*, Assumption 2^* with $y = 1$), and $\mathrm{CIE}_1 \leq P_{1,111} - P_{1,101}$ under Assumption 1^* and $\beta_{11} \geq 0$ (*i.e.*, Assumption 2^{**} with $y = 1$). Therefore, similar to Results 1, 2 and 3 imply that we can derive both bounds for CIE_1 and CIE_2 under slightly stronger assumptions than theirs.

References

Angrist, J.D., Imbens, G.W., Rubin, D.B., 1996. Identification of causal effects using instrumental variables. J. Amer. Statist. Assoc. 91, 444–455.
Cheng, J., Small, D.S., 2006. Bounds on causal effects in three-arm trials with non-compliance. J. R. Stat. Soc. Ser. B 68, 815–836.
Chiba, Y., 2010. Bias analysis for the principal stratum direct effect in the presence of confounded intermediate variables. J. Biomet. Biostat. 1, 101.
Chiba, Y., 2012a. The large sample bounds on the principal strata effect with application to a prostate cancer prevention trial. Int. J. Biostat. (in press).
Chiba, Y., 2012b. Bounds on the complier average causal effect in randomized trials with noncompliance. Stat. Probabil. Lett., in this issue (http://dx.doi.org/10.1016/j.spl.2012.03.040).
Chiba, Y., VanderWeele, T.J., 2011. A simple method for principal strata effects when the outcome has been truncated due to death. Am. J. Epidemiol. 173, 745–751.
Dawid, A.P., 2000. Causal inference without counterfactuals. J. Amer. Statist. Assoc. 95, 407–424.
Frangakis, C.E., Rubin, D.B., 2002. Principal stratification in causal inference. Biometrics 58, 21–29.
Halloran, M.E., Hudgens, M.G., 2012. Causal inference for vaccine effects on infectiousness. Int. J. Biostat. 8 (2), 6.
Halloran, M.E., Struchiner, C.J., 1991. Study designs for dependent happenings. Epidemiology 2, 331–338.
Halloran, M.E., Struchiner, C.J., 1995. Causal inference for infectious diseases. Epidemiology 6, 142–151.
Hong, G., Raudenbush, S.W., 2006. Evaluating kindergarten retention policy: a case study of causal inference for multilevel observational data. J. Amer. Statist. Assoc. 101, 901–910.
Hudgens, M.G., Halloran, M.E., 2006. Causal vaccine effects on binary post-infection outcomes. J. Amer. Statist. Assoc. 101, 51–64.
Hudgens, M.G., Halloran, M.E., 2008. Towards causal inference with interference. J. Amer. Statist. Assoc. 103, 832–842.
Little, R.J., Rubin, D.B., 2000. Causal effects in clinical and epidemiological studies via potential outcomes: concepts and analytical approaches. Annu. Rev. Public Health 21, 121–145.
Pearl, J., 2009. Causality: Models, Reasoning, and Inference, second ed. Cambridge University Press.
Rosenbaum, P.R., 1984. The consequences of adjustment for a concomitant variable that has been affected by the treatment. J. R. Stat. Soc. Ser. A 147, 656–666.
Rosenbaum, P.R., 2007. Interference between units in randomized experiments. J. Amer. Statist. Assoc. 102, 191–200.
Rubin, D.B., 2004. Direct and indirect causal effects via potential outcomes. Scand. J. Stat. 31, 161–170.
Sobel, M.E., 2006. What do randomized studies of housing mobility demonstrate? Causal inference in the face of interference. J. Amer. Statist. Assoc. 101, 1398–1407.
Tchetgen Tchetgen, E.J., VanderWeele, T.J., 2012. Estimation of causal effects in the presence of interference. Stat. Methods Med. Res. 21, 55–75.
VanderWeele, T.J., 2010. Direct and indirect effects for neighborhood-based clustered and longitudinal data. Sociol. Methods Res. 38, 515–544.
VanderWeele, T.J., Tchetgen Tchetgen, E.J., 2011. Bounding the infectiousness effect in vaccine trials. Epidemiology 22, 686–693.
Zhang, J.L., Rubin, D.B., 2003. Estimation of causal effects via principal stratification when some outcomes are truncated by death. J. Educ. Behav. Stat. 28, 353–368.
Zhang, J., Rubin, D.B., Mealli, F., 2008. Evaluating the effects of job training programs on wages through principal stratification. In: Millimet, D., Smith, J., Vytlacil, E. (Eds.), Advances in Econometrics: Modelling and Evaluating Treatment Effects in Econometrics. Elsevier Science, pp. 117–145.